



Research article

Topological optimization algorithm for mechanical-electrical coupling of periodic composite materials

Ziqiang Wang, Chunyu Cen and Junying Cao*

School of Data Science and Information Engineering, Guizhou Minzu University, Guiyang 550025, China

* **Correspondence:** Email: caojunying@gzmu.edu.cn.

Abstract: In this paper, a topology optimization algorithm for the mechanical-electrical coupling problem of periodic composite materials is studied. Firstly, the homogenization problem of the mechanical-electrical coupling topology optimization problem of periodic composite materials is established by the multi-scale asymptotic expansion method. Secondly, the topology optimization algorithm for the mechanical-electrical coupling problem of periodic composite materials is constructed by finite element method, solid isotropic material with penalisation method and homogenization method. Finally, numerical results show that the proposed algorithm is effective to calculate the optimal structure of the periodic composite cantilever beam under the influence of the mechanical-electrical coupling.

Keywords: mechanical-electrical coupling; composite materials; solid isotropic material method; homogenization method

1. Introduction

Structural optimization of piezoelectric composites is one of the hot issues in structural design of materials. Piezoelectric composites are widely used in aircraft structure, electronic information technology and semiconductor materials [1,2]. Composite materials generally have some small periodicity, which makes it difficult to solve the differential equations that describe piezoelectric problems theoretically. For piezoelectric phenomena of composite structures, a simple and effective algorithm is developed based on the idea of homogenization [3, 4]. In [5], the homogenization method is used to establish a numerical algorithm for calculating the optimal design of composite structures. In [6], mainly presented a multi-scale and multi-material topology optimization algorithm for designing cellular structure. The reference [7] proposed a topology optimization method for structural heat transfer and load carrying capabilities. The optimal structure and microstructure topology optimization meth-

ods of materials are presented in [8]. In [9], a piezoelectric plate energy harvester of in-plane harmonic energy is studied, and proposed a topology optimization algorithm of two-dimensional piezoelectric material model, which minimizes the numerical instability. A topology optimization algorithm is proposed based on probabilistic reliability for piezoelectric uncertainty, and established a nested double-loop optimization algorithm to satisfy the displacement performance in [10]. For multi-scale structural topology optimization, in [11], mainly studies a two-scale concurrent topology optimization design of multi-micro heterogeneous materials. The two-scale design optimization problem of minimizing structural compliance under the constraints of seepage flow rate and material void is studied in [12]. In [13], a hierarchical topology optimization design method applied to single scale microstructure of mechanical materials is proposed. The finite element method is introduced through the homogenization method of composite materials, and the homogenization constant of composite materials is realized by the program [14–16]. A structure-material design two-scale optimization methods in the framework of level set method presented in [17]. In reference [18, 19] proposed a topology optimization design method for solids and fluids periodicity and microstructure of porous materials. In [20], based on the multi-material topology optimization, some materials with fully combined bi-functions are developed and proposed a method for selecting reasonable parameters. A topology optimization algorithm to improve the alternating active phase and object of multiple materials and a new formula to overcome convergent oscillations are presented in [21]. A two-scale parallel optimization method is proposed and applied to the macroscopic and microscopic structures, finally, compared the optimized gradient and uniform graded lattice structures in [22]. In [23], mainly proposed a multi-material topology optimization algorithm and candidate material selection criteria, and applied the topology optimization algorithm to the compliance minimization problem. In [24], this paper mainly studies the bending behavior of three-dimensional periodic composite plates and designs a two-scale computing method, which is used to solve the effective parameters and displacement strains of the composite plates. A method of constructing a higher order scheme for numerical solutions of the fractional ordinary differential equations is proposed in [25]. The high-order numerical scheme of caputo time fractional differential equation with uniform accuracy is constructed by constructing high-order finite difference method and local truncation error in [26]. An effective topology optimization method for macrostructure and their corresponding parameterized microstructure is presented in [27]. In [28], a topology optimization algorithm based on level set composites is proposed, and the algorithm is applied to the compliance minimization of linear elastic problems. It established a two-scale coupling relationship between potential and displacement and analyzed some improved asymptotic error estimates in [29]. The structure optimization algorithm of piezoelectric material plate is established by moving asymptote method, and the program experiment is given by Matlab in [30]. For more practical applications, see [31, 32].

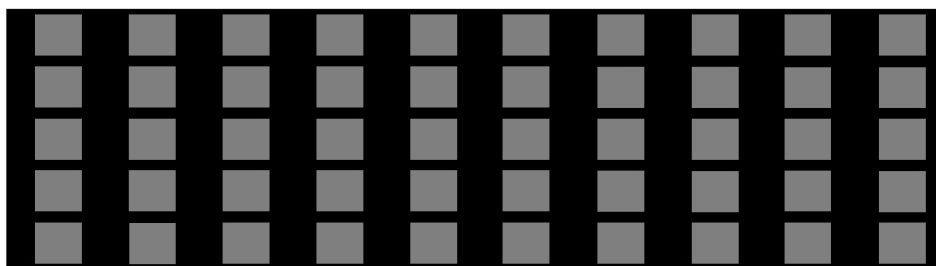
According to the current literature research, there are few mechanical-electrical coupling topology optimization algorithms for piezoelectric composites. This paper constructs a structural optimization algorithm for the electro-mechanical coupling problem of composite materials based on the two-scale asymptotic expansion method. The algorithm is used to calculate the optimization problem of cantilever beam structure. This paper is arranged as follows: construction and analysis of topological optimization method for electro-mechanical coupling problems of periodic composite materials in Section 2. In Section 3, establish a topological optimization algorithm for the electro-mechanical coupling problem of periodic composite materials, and the topology optimization structure of fine mesh and

homogenized solution were compared. Finally, some conclusions are given in Section 4.

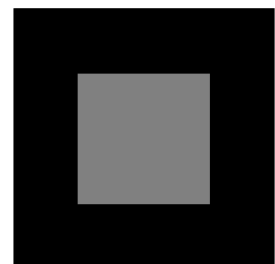
Nomenclature			
List of Symbols			
E^ε	Young's modulus(N/m ²)	ρ	Density(kg/m ³)
E_0^ε	Young's modulus for void materials(N/m ²)	$\lambda^\varepsilon, \mu^\varepsilon$	Lame constants
E_1^ε	Young's modulus for solid materials(N/m ²)	f_i	Body forces(N)
$C_{ijhk}^{\theta, \varepsilon}$	Elastic constant(N/m ²)	u_k^ε	Displacement field(m)
$C_{ijhk(0)}^{\theta, \varepsilon}$	Elastic constant for void materials(N/m ²)	t_i	Surface load(N)
$C_{ijhk(1)}^{\theta, \varepsilon}$	Elastic constant for solid materials(N/m ²)	θ	Design variable
$e_{ijk}^{\theta, \varepsilon}$	Piezoelectric constant(C/m ²)	ν	Poisson's ratio
$e_{ijk(0)}^{\theta, \varepsilon}$	Piezoelectric constant for void materials(C/m ²)	G	Original sensitivity
$e_{ijk(1)}^{\theta, \varepsilon}$	Piezoelectric constant for solid materials(C/m ²)	G_r	Smoothed sensitivity
$b_{ij}^{\theta, \varepsilon}$	Dielectric constant(F/m)	δG_r	The variation of G_r
$b_{ij(0)}^{\theta, \varepsilon}$	Dielectric constant for void materials (F/m)	γ_i	Positive constant
$b_{ij(1)}^{\theta, \varepsilon}$	Dielectric constant for solid materials(F/m)	$\chi_k, \bar{\lambda}, \phi$	Lagrange multiplier
Φ^ε	Electric potential field(V)	$move$	Density change
p	Penalization factor	η	Damping coefficient
q	Concentrated electric loads(C)	ϑ	Volume constraint
$K^{h_0}(Y)$	Finite element spaces	$K^{h_1}(Y)$	Finite element spaces

2. Construction and analysis of topological optimization method for mechanical-electrical coupling problems of periodic composite materials

Suppose a cantilever beams with length W and width L were considered in the simulations. As shown in Figure 1, let Ω be a bounded domain with Lipschitz boundary. In what follows, Latin indices take numbers in 1, 2, 3, while Greek ones only run over 1, 2. In addition, we shall constantly use the Einstein summation convention.



a. Composite materials domain Ω .



b. Monocellular domain Y .

Figure 1. Initial material.

The famous material interpolation schemes is the density-based method. For non-isotropic piezoelectric material, the interpolation function is the extension of solid isotropic microstructure with pe-

nalization (SIMP) scheme which can be written as follows:

$$\begin{aligned}
 E^\varepsilon(x) &= E_0^\varepsilon(x) + (E_1^\varepsilon(x) - E_0^\varepsilon(x))\theta^p(x), \\
 C_{ijhk}^{\theta,\varepsilon}(x) &= C_{ijhk(0)}^{\theta,\varepsilon}(x) + (C_{ijhk(1)}^{\theta,\varepsilon}(x) - C_{ijhk(0)}^{\theta,\varepsilon}(x))\theta^p(x), \\
 e_{kij}^{\theta,\varepsilon}(x) &= e_{kij(0)}^{\theta,\varepsilon}(x) + (e_{kij(1)}^{\theta,\varepsilon}(x) - e_{kij(0)}^{\theta,\varepsilon}(x))\theta^p(x), \\
 b_{ij}^{\theta,\varepsilon}(x) &= b_{ij(0)}^{\theta,\varepsilon}(x) + (b_{ij(1)}^{\theta,\varepsilon}(x) - b_{ij(0)}^{\theta,\varepsilon}(x))\theta^p(x).
 \end{aligned} \tag{2.1}$$

It is noted that the parameter $\theta(x)$ is a design variable. Similarly, the Lamé parameters describing the mechanical properties of a solid can be expressed as follows:

$$\lambda^\varepsilon(x) = \frac{\nu E^\varepsilon(x)}{(1+\nu)(1-2\nu)}, \quad \mu^\varepsilon(x) = \frac{E^\varepsilon(x)}{2(1+\nu)}. \tag{2.2}$$

Consider the following minimization of mechanical-electrical coupling problem for two-dimensional periodic composite materials, the objective function is described as:

$$\begin{aligned}
 \min_{\theta} J(\theta) &= \int_{\Omega} f_i(x)u_i^\varepsilon(x)\theta(x) dx + \int_{B_t} t_i(x)u_i^\varepsilon(x) ds \\
 &\quad - \int_{\Omega} \rho(x)\Phi^\varepsilon(x)\theta(x) dx - \int_{B_\phi} q(x)\Phi^\varepsilon(x) ds,
 \end{aligned} \tag{2.3}$$

subject to

$$\left\{ \begin{aligned}
 &-\frac{\partial}{\partial x_j} \left(C_{ijkl}^{\theta,\varepsilon}(x) \frac{\partial u_k^\varepsilon(x)}{\partial x_l} + e_{kij}^{\theta,\varepsilon}(x) \frac{\partial \Phi^\varepsilon(x)}{\partial x_k} \right) = f_i(x)\theta(x), \quad \text{in } \Omega, \\
 &-\frac{\partial}{\partial x_i} \left(b_{ij}^{\theta,\varepsilon}(x) \frac{\partial \Phi^\varepsilon(x)}{\partial x_j} - e_{ijk}^{\theta,\varepsilon}(x) \frac{\partial u_k^\varepsilon(x)}{\partial x_j} \right) = \rho(x)\theta(x), \quad \text{in } \Omega, \\
 &u_k^\varepsilon(x) = 0, \quad \text{on } B_u, \\
 &\left(\frac{\partial u_k^\varepsilon(x)}{\partial x_l} C_{ijkl}^{\theta,\varepsilon}(x) + e_{kij}^{\theta,\varepsilon}(x) \frac{\partial \Phi^\varepsilon(x)}{\partial x_k} \right) n_j = t_i(x), \quad \text{on } B_t, \\
 &\left(\frac{\partial \Phi^\varepsilon(x)}{\partial x_j} b_{ij}^{\theta,\varepsilon}(x) - e_{ijk}^{\theta,\varepsilon}(x) \frac{\partial u_k^\varepsilon(x)}{\partial x_j} \right) n_i = q(x), \quad \text{on } B_\phi, \\
 &\Phi^\varepsilon(x) = 0, \quad \text{on } B_q, \\
 &\int_{\Omega} \theta(x) dx / |\Omega| \leq \vartheta, 0 \leq \theta(x) \leq 1,
 \end{aligned} \right. \tag{2.4}$$

where $f_i(x)$ is the body force, $\rho(x)$ is the density of charge, ϑ is volume constraint, \mathbf{n} is a normal vector, $u_k^\varepsilon(x)$ is the displacement vector, $\Phi^\varepsilon(x)$ is the scalar electric potential field, $t_i(x)$ is surface traction force, $q(x)$ denotes the electric body charge, and the boundary $\partial\Omega$ of Ω is composed of the traction boundary B_t and the displacement boundary B_u with $B_u \cap B_t = 0$ and $B_u \cup B_t = \partial\Omega$. Similarly, the electrical boundary Ω is divided into two parts, the electric potential boundary B_ϕ and the electric loads boundary B_q with $B_\phi \cap B_q = 0$ and $B_\phi \cup B_q = \partial\Omega$.

Assume that all coefficients satisfy the following conditions

$$\text{(I) } C_{ijhk}^{\theta,\varepsilon}(x) = C_{ijhk}^\theta(\xi), e_{ijk}^{\theta,\varepsilon}(x) = e_{ijk}^\theta(\xi), b_{ij}^{\theta,\varepsilon}(x) = b_{ij}^\theta(\xi) \text{ is periodic } Y \text{ and } \xi = x/\varepsilon;$$

(II) $C_{ijhk}^{\theta,\varepsilon}(x)$ satisfies the following coercive condition $\Xi(k_1, k_2)$, s.t.,

$$\begin{cases} C_{ijhk}^{\theta,\varepsilon}(x) = C_{jikh}^{\theta,\varepsilon}(x) = C_{ijkh}^{\theta,\varepsilon}(x), \\ k_1 \zeta_{ih} \zeta_{ih} \leq C_{ijhk}^{\theta,\varepsilon}(x) \zeta_{ih} \zeta_{jk} \leq k_2 \zeta_{jk} \zeta_{jk}, \end{cases}$$

where $\{\zeta_{ih}\}$ is real elements with arbitrary symmetric matrix, k_1 and k_2 are positive constants independent of ε ;

(III) $b_{ij}^{\theta,\varepsilon}(x)$ satisfies the following positive definite condition:

$$b_{ij}^{\theta,\varepsilon}(x) = b_{ji}^{\theta,\varepsilon}(x), \quad \tau_1 \zeta_i \zeta_i \leq b_{ij}^{\theta,\varepsilon}(x) \zeta_i \zeta_j \leq \tau_2 \zeta_j \zeta_j,$$

where $\{\zeta_i\}$ is an arbitrary vector with real element, τ_1 and τ_2 are constants greater than zero independent of ε ;

(IV) For tensor $e_{ijk}^{\theta,\varepsilon}(x)$, we assume that $e_{ijk}^{\theta,\varepsilon}(x) = e_{ikj}^{\theta,\varepsilon}(x)$.

Theorem 2.1. Assume that the homogenization coefficients \hat{C}_{ijhk}^θ , \hat{e}_{ijk}^θ and \hat{b}_{ij}^θ satisfy the conditions (I)–(IV), then the homogenization problem of Eq (2.3) is as follows:

$$\min_{\theta} J(\theta) = \int_{\Omega} f_i(x) u_i^0(x) \theta(x) dx + \int_{B_t} t_i(x) u_i^0(x) ds - \int_{\Omega} \rho(x) \Phi^0(x) \theta(x) dx - \int_{B_\phi} q(x) \Phi^0(x) ds,$$

and satisfy the following equations

$$\begin{cases} -\frac{\partial}{\partial x_j} \left(\hat{C}_{ijkl}^\theta \frac{\partial u_k^0(x)}{\partial x_l} + \hat{e}_{kij}^\theta \frac{\partial \Phi^0(x)}{\partial x_k} \right) = f_i(x) \theta(x), & \text{in } \Omega, \\ -\frac{\partial}{\partial x_i} \left(\hat{b}_{ij}^\theta \frac{\partial \Phi^0(x)}{\partial x_j} - \hat{e}_{ijk}^\theta \frac{\partial u_k^0(x)}{\partial x_j} \right) = \rho(x) \theta(x), & \text{in } \Omega, \\ u_k^0(x) = 0, & \text{on } B_u, \\ \left(\hat{C}_{ijkl}^\theta \frac{\partial u_k^0(x)}{\partial x_l} + \hat{e}_{kij}^\theta \frac{\partial \Phi^0(x)}{\partial x_k} \right) n_j = t_i(x), & \text{on } B_t, \\ \left(\hat{b}_{ij}^\theta \frac{\partial \Phi^0(x)}{\partial x_j} - \hat{e}_{ijk}^\theta \frac{\partial u_k^0(x)}{\partial x_j} \right) n_i = q(x), & \text{on } B_\phi, \\ \Phi^0(x) = 0, & \text{on } B_q, \\ \int_{\Omega} \theta(x) dx / |\Omega| \leq \vartheta, 0 \leq \theta(x) \leq 1. \end{cases} \quad (2.5)$$

Let's define the coefficients of homogenization \hat{C}_{ijhk}^θ , \hat{e}_{ijk}^θ and \hat{b}_{ij}^θ as follows:

$$\hat{C}_{ijhk}^\theta = \frac{1}{|Y|} \int_Y \left[C_{ijhk}^\theta(\xi) + C_{ijlm}^\theta(\xi) \frac{\partial (N_{hk}(\xi))_l}{\partial \xi_m} + e_{lij}^\theta(\xi) \frac{\partial G_{hk}(\xi)}{\partial \xi_l} \right] d\xi, \quad (2.6)$$

$$\hat{e}_{ijk}^\theta = \frac{1}{|Y|} \int_Y \left[e_{ijk}^\theta(\xi) + C_{ijlm}^\theta(\xi) \frac{\partial (M_k(\xi))_l}{\partial \xi_m} + e_{lij}^\theta(\xi) \frac{\partial H_k(\xi)}{\partial \xi_l} \right] d\xi, \quad (2.7)$$

$$\hat{b}_{ij}^\theta = \frac{1}{|Y|} \int_Y \left[b_{ij}^\theta(\xi) - e_{itm}^\theta(\xi) \frac{\partial (M_j(\xi))_l}{\partial \xi_m} + b_{ik}^\theta(\xi) \frac{\partial H_j(\xi)}{\partial \xi_k} \right] d\xi, \quad (2.8)$$

where $H(\xi), G(\xi), M(\xi), N(\xi)$ are Y -periodic in ξ and defined by as follows

$$\begin{cases} \frac{\partial}{\partial \xi_j} \left(e_{kij}^\theta(\xi) \frac{\partial H_{\alpha_1}(\xi)}{\partial \xi_k} \right) + \frac{\partial}{\partial \xi_j} \left(C_{ijhk}^\theta(\xi) \frac{\partial (M_{\alpha_1}(\xi))_h}{\partial \xi_k} \right) + \frac{\partial}{\partial \xi_j} \left(e_{\alpha_1 ij}^\theta(\xi) \right) = 0, & \text{in } \Omega, \\ \frac{\partial}{\partial \xi_i} \left(-b_{ij}^\theta(\xi) \frac{\partial H_{\alpha_1}(\xi)}{\partial \xi_j} \right) + \frac{\partial}{\partial \xi_i} \left(e_{ikj}^\theta(\xi) \frac{\partial (M_{\alpha_1}(\xi))_k}{\partial \xi_j} \right) - \frac{\partial}{\partial \xi_i} \left(b_{\alpha_1 i}^\theta(\xi) \right) = 0, & \text{in } \Omega, \\ \int_{\Omega} M_{\alpha_1}(\xi) d\xi = 0, \int_{\Omega} H_{\alpha_1}(\xi) d\xi = 0, \end{cases} \quad (2.9)$$

and

$$\begin{cases} \frac{\partial}{\partial \xi_j} \left(C_{ijhk}^\theta(\xi) \frac{\partial (N_{\alpha_1 m}(\xi))_h}{\partial \xi_k} \right) + \frac{\partial}{\partial \xi_j} \left(C_{ij\alpha_1 m}^\theta(\xi) \right) + \frac{\partial}{\partial \xi_j} \left(e_{kij}^\theta(\xi) \frac{\partial G_{\alpha_1 m}(\xi)}{\partial \xi_k} \right) = 0, & \text{in } \Omega, \\ \frac{\partial}{\partial \xi_i} \left(-b_{ij}^\theta(\xi) \frac{\partial G_{\alpha_1 m}(\xi)}{\partial \xi_j} \right) + \frac{\partial}{\partial \xi_i} \left(e_{ikj}^\theta(\xi) \frac{\partial (N_{\alpha_1 m}(\xi))_k}{\partial \xi_j} \right) + \frac{\partial}{\partial \xi_i} \left(e_{i\alpha_1}^\theta(\xi) \right) = 0, & \text{in } \Omega, \\ \int_{\Omega} N_{\alpha_1 m}(\xi) d\xi = 0, \int_{\Omega} G_{\alpha_1 m}(\xi) d\xi = 0. \end{cases} \quad (2.10)$$

Proof. For a detailed proof, see Appendix A.

The sensitivity analysis is derived by the Lagrange multiplier L , for the optimization problem of mechanical-electrical coupling of the discussed composite materials, the Lagrange multiplier can be defined as:

$$\begin{aligned} L(\bar{u}^0(x), \bar{\Phi}^0(x), \theta(x), \bar{\chi}(x), \bar{\phi}(x)) &= J(\theta) - \int_{\Omega} f_i(x) \bar{\chi}_i(x) \theta(x) dx - \int_{B_r} t_i(x) \bar{\chi}_i(x) ds \\ &+ \int_{\Omega} \rho(x) \bar{\phi}(x) \theta(x) dx + \int_{\Omega} (\hat{e}_{kij}^\theta(\xi) \frac{\partial \bar{\Phi}^0(x)}{\partial x_i}) \frac{\partial \bar{\chi}_k(x)}{\partial x_j} dx + \int_{\Omega} (\hat{e}_{ijk}^\theta(\xi) \frac{\partial \bar{u}_k^0(x)}{\partial x_j}) \frac{\partial \bar{\phi}(x)}{\partial x_i} dx \\ &+ \int_{\Omega} (\hat{C}_{ijkl}^\theta(\xi) \frac{\partial \bar{u}_k^0(x)}{\partial x_l}) \frac{\partial \bar{\chi}_i(x)}{\partial x_j} dx + \int_{B_\phi} q(x) \bar{\phi}(x) ds - \int_{\Omega} (\hat{b}_{ij}^\theta(\xi) \frac{\partial \bar{\Phi}^0(x)}{\partial x_j}) \frac{\partial \bar{\phi}(x)}{\partial x_i} dx, \end{aligned} \quad (2.11)$$

where $(\bar{u}^0(x), \bar{\chi}(x)) \in U$ is a vector-valued function, $\bar{\chi}(x)$ is the Lagrange multiplier of the governing equation and the Neumann boundary condition on B_r , $(\bar{\Phi}^0(x), \bar{\phi}(x)) \in Z$ is a quantity-valued function, $\bar{\phi}(x)$ is the Lagrange multiplier of the governing equation and the Neumann boundary condition on B_ϕ . The dual spaces of U and Z are U' and Z' , respectively.

Theorem 2.2. Suppose $\bar{u}_k^0(x) \in U$ and $\bar{\Phi}^0(x) \in Z$ are locally optimal solutions of (2.5), then there are $\chi_k(x) \in U'$ and $\phi(x) \in Z'$, both of which satisfied the following conditions:

$$\begin{cases} \frac{\partial}{\partial x_j} \left(\hat{C}_{ijkl}^\theta \frac{\partial \chi_k(x)}{\partial x_l} + \hat{e}_{ijk}^\theta \frac{\partial \phi(x)}{\partial x_k} \right) = f_i(x) \theta(x), & \text{in } \Omega, \\ \frac{\partial}{\partial x_i} \left(\hat{b}_{ij}^\theta \frac{\partial \phi(x)}{\partial x_j} - \hat{e}_{kij}^\theta \frac{\partial \chi_k(x)}{\partial x_j} \right) = \rho(x) \theta(x), & \text{in } \Omega, \\ \chi_k(x) = 0, & \text{on } B_u, \\ - \left(\hat{C}_{ijkl}^\theta \frac{\partial \chi_k(x)}{\partial x_l} + \hat{e}_{ijk}^\theta \frac{\partial \phi(x)}{\partial x_k} \right) n_j = t_i(x), & \text{on } B_r, \\ - \left(\hat{b}_{ij}^\theta \frac{\partial \phi(x)}{\partial x_j} - \hat{e}_{kij}^\theta \frac{\partial \chi_k(x)}{\partial x_j} \right) n_i = q(x), & \text{on } B_\phi, \\ \phi(x) = 0, & \text{on } B_q. \end{cases} \quad (2.12)$$

Proof. The partial derivative of Eq (2.11) with respect to $\bar{u}_k^0(x)$ in the direction $\delta\bar{u}_k^0(x)$ at a stationary point $(u_k^0(x), \chi_k(x)) \in U$ leads to

$$\begin{aligned} \left\langle \frac{\partial L}{\partial \bar{u}_k^0(x)} \left(u^0(x), \Phi^0(x), \theta(x), \chi(x), \phi(x) \right), \delta\bar{u}_k^0(x) \right\rangle &= \int_{B_t} t_k(x) \delta\bar{u}_k^0(x) ds + \int_{\Omega} f_k(x) \delta\bar{u}_k^0(x) \theta(x) dx \\ &+ \int_{\Omega} (\hat{C}_{ijkl}^{\theta}(\xi) \frac{\partial}{\partial x_l} \delta\bar{u}_k^0(x)) \frac{\partial \chi_i(x)}{\partial x_j} dx + \int_{\Omega} (\hat{e}_{ijk}^{\theta}(\xi) \frac{\partial}{\partial x_j} \delta\bar{u}_k^0(x)) \frac{\partial \phi(x)}{\partial x_i} dx = 0. \end{aligned} \quad (2.13)$$

Similarly, taking the derivative of Eq (2.11) with respect to $\bar{\Phi}^0(x)$ in the direction $\delta\bar{\Phi}^0(x)$ at a stationary point $(\Phi^0(x), \phi(x)) \in Z$ leads to

$$\begin{aligned} \left\langle \frac{\partial L}{\partial \bar{\Phi}^0(x)} \left(u^0(x), \Phi^0(x), \theta(x), \chi(x), \phi(x) \right), \delta\bar{\Phi}^0(x) \right\rangle &= - \int_{\Omega} \rho(x) \delta\bar{\Phi}^0(x) \theta(x) dx - \int_{B_{\phi}} q(x) \delta\bar{\Phi}^0(x) ds \\ &- \int_{\Omega} (\hat{b}_{ij}^{\theta}(\xi) \frac{\partial}{\partial x_j} \delta\bar{\Phi}^0(x)) \frac{\partial \phi(x)}{\partial x_i} dx + \int_{\Omega} (\hat{e}_{kij}^{\theta}(\xi) \frac{\partial}{\partial x_i} \delta\bar{\Phi}^0(x)) \frac{\partial \chi_k(x)}{\partial x_j} dx = 0. \end{aligned} \quad (2.14)$$

In the third term on the right hand side of (2.13) and (2.14), $\delta\bar{u}_k^0(x)$ can commute with $\chi_k(x)$ and $\delta\bar{\Phi}^0$ commute with $\phi(x)$ due to the symmetric property of the bilinear form, i.e.,

$$\left(\hat{C}_{ijkl}^{\theta}(\xi) \frac{\partial \delta\bar{u}_k^0(x)}{\partial x_l} \right) \frac{\partial \chi_i(x)}{\partial x_j} = \left(\hat{C}_{ijkl}^{\theta}(\xi) \frac{\partial \chi_i(x)}{\partial x_j} \right) \frac{\partial \delta\bar{u}_k^0(x)}{\partial x_l}, \quad (2.15)$$

$$\left(\hat{b}_{ij}^{\theta}(\xi) \frac{\partial \delta\bar{\Phi}^0(x)}{\partial x_j} \right) \frac{\partial \phi(x)}{\partial x_i} = \left(\hat{b}_{ij}^{\theta}(\xi) \frac{\partial \phi(x)}{\partial x_i} \right) \frac{\partial \delta\bar{\Phi}^0(x)}{\partial x_j}. \quad (2.16)$$

Substituting (2.15) into (2.13) and (2.16) into (2.14) and taking integration by parts lead to the following equation

$$\begin{aligned} \left\langle \frac{\partial L}{\partial \bar{u}_k^0} \left(u^0(x), \Phi^0(x), \theta(x), \chi(x), \phi(x) \right), \delta\bar{u}_k^0(x) \right\rangle &= \int_{\Omega} f_k(x) \theta(x) \delta\bar{u}_k^0(x) dx + \int_{B_t} t_k(x) \delta\bar{u}_k^0(x) ds \\ &+ \int_{B_t} n_j (\hat{C}_{ijkl}^{\theta}(\xi) \frac{\partial \chi_i(x)}{\partial x_j}) \delta\bar{u}_k^0(x) ds + \int_{B_t} n_j (\hat{e}_{ijk}^{\theta}(\xi) \frac{\partial \phi(x)}{\partial x_i}) \delta\bar{u}_k^0(x) ds \\ &- \int_{\Omega} \frac{\partial}{\partial x_l} (\hat{C}_{ijkl}^{\theta}(\xi) \frac{\partial \chi_i(x)}{\partial x_j}) \delta\bar{u}_k^0(x) dx - \int_{\Omega} \frac{\partial}{\partial x_j} (\hat{e}_{ijk}^{\theta}(\xi) \frac{\partial \phi(x)}{\partial x_i}) \delta\bar{u}_k^0(x) dx = 0, \end{aligned} \quad (2.17)$$

and

$$\begin{aligned} \left\langle \frac{\partial L}{\partial \bar{\Phi}^0(x)} \left(u^0(x), \Phi^0(x), \theta(x), \chi(x), \phi(x) \right), \delta\bar{\Phi}^0(x) \right\rangle &= - \int_{\Omega} \rho(x) \theta(x) \delta\bar{\Phi}^0(x) dx - \int_{B_{\phi}} q(x) \delta\bar{\Phi}^0(x) ds \\ &+ \int_{\Omega} \frac{\partial}{\partial x_i} (\hat{b}_{ij}^{\theta}(\xi) \frac{\partial \phi(x)}{\partial x_j}) \delta\bar{\Phi}^0(x) dx - \int_{\Omega} \frac{\partial}{\partial x_i} (\hat{e}_{kij}^{\theta}(\xi) \frac{\partial \chi_k(x)}{\partial x_j}) \delta\bar{\Phi}^0(x) dx \\ &- \int_{B_{\phi}} n_j (\hat{b}_{ij}^{\theta}(\xi) \frac{\partial \phi(x)}{\partial x_i}) \delta\bar{\Phi}^0(x) ds + \int_{B_{\phi}} n_i (\hat{e}_{kij}^{\theta}(\xi) \frac{\partial \chi_k(x)}{\partial x_j}) \delta\bar{\Phi}^0(x) ds = 0. \end{aligned} \quad (2.18)$$

For arbitrarily function $\bar{u}_k^0(x) \in U$ and $\bar{\Phi}^0(x) \in Z$ are locally optimal solutions of (2.5). Theorem 2.2 has been proved.

The finite element method is used to solve the adjoint Eq (2.12) to obtain $\chi_k(x)$ and $\phi(x)$, which are substituted into $J(\theta)$. The sensitivity of the objective function is obtained by taking the derivative of

$$J(\theta) = L(u^0(x), \Phi^0(x), \theta(x), \chi(x), \phi(x)). \quad (2.19)$$

With take the derivative of the design variable θ :

$$\begin{aligned} \left\langle \frac{\partial J}{\partial \theta}, \delta \theta \right\rangle &= \int_{\Omega} \left[f_i(x) u_i^0(x) + \left(\frac{\partial \hat{C}_{ijkl}^{\theta}(\xi)}{\partial \theta} \frac{\partial u_k^0(x)}{\partial x_l} \right) \frac{\partial \chi_i(x)}{\partial x_j} - \rho(x) \Phi^0(x) \right. \\ &\quad + \left(\frac{\partial \hat{e}_{kij}^{\theta}(\xi)}{\partial \theta} \frac{\partial \Phi^0(x)}{\partial x_i} \right) \frac{\partial \chi_k(x)}{\partial x_j} - \left(\frac{\partial \hat{b}_{ij}^{\theta}(\xi)}{\partial \theta} \frac{\partial \Phi^0(x)}{\partial x_j} \right) \frac{\partial \phi(x)}{\partial x_i} + \rho(x) \phi(x) \\ &\quad \left. + \left(\frac{\partial \hat{e}_{ijk}^{\theta}(\xi)}{\partial \theta} \frac{\partial u_k^0(x)}{\partial x_j} \right) \frac{\partial \phi(x)}{\partial x_i} - f_i(x) \chi_i(x) \right] \delta \theta dx = \int_{\Omega} \frac{\partial J}{\partial \theta} \delta \theta dx. \end{aligned}$$

Then the objective function of the sensitivity analysis is following as:

$$\begin{aligned} \frac{\partial J}{\partial \theta} &= f_i(x) u_i^0(x) - \rho(x) \Phi^0(x) + \left(\frac{\partial \hat{C}_{ijkl}^{\theta}(\xi)}{\partial \theta} \frac{\partial u_k^0(x)}{\partial x_l} \right) \frac{\partial \chi_i(x)}{\partial x_j} - f_i(x) \chi_i(x) + \rho(x) \phi(x) \\ &\quad + \left(\frac{\partial \hat{b}_{ij}^{\theta}(\xi)}{\partial \theta} \frac{\partial \Phi^0(x)}{\partial x_j} \right) \frac{\partial \phi(x)}{\partial x_i} - \left(\frac{\partial \hat{e}_{kij}^{\theta}(\xi)}{\partial \theta} \frac{\partial \Phi^0(x)}{\partial x_i} \right) \frac{\partial \chi_k(x)}{\partial x_j} + \left(\frac{\partial \hat{e}_{ijk}^{\theta}(\xi)}{\partial \theta} \frac{\partial u_k^0(x)}{\partial x_j} \right) \frac{\partial \phi(x)}{\partial x_i}. \end{aligned} \quad (2.20)$$

In order to ensure that checkerboard patterns are avoided in the solution of topology optimization problems, some design constraints must be limited. This situation can be eliminated by smoothing sensitivity of objective function $J(\theta)$ and material volume V is given by the following equation:

$$\int_{\Omega} \left(\gamma_i \frac{\partial G_r}{\partial x_i} \frac{\partial}{\partial x_r} (\delta G_r) + G_r (\delta G_r) \right) dx = \int_{\Omega} G (\delta G_r) dx, \quad (2.21)$$

where G_r and G are the smoothed and original densities, respectively. δG_r is the variation of G_r , γ_i is a positive constant. Considering only the volume constraint, the structural optimization problem of Eq (2.19) can be expressed as:

$$\min_{\theta} J(\theta) \quad \text{s.t.} \quad \int_{\Omega} \theta dx / |\Omega| \leq \vartheta, \theta_{min} \leq \theta \leq 1. \quad (2.22)$$

For the constraint conditions of Eq (2.22), the necessary condition for θ to be optimal is satisfying that a subset of the stability condition of the Lagrange function, so we use the Lagrange multiplier Λ , λ_1 and λ_2 . Then, we have:

$$\tilde{L}(\theta, \Lambda, \bar{\lambda}_1, \bar{\lambda}_2) = \Lambda \left(\int_{\Omega} \theta dx / |\Omega| - \vartheta \right) + \int_{\Omega} \bar{\lambda}_1 (\theta_{min} - 1) dx + \int_{\Omega} \bar{\lambda}_2 (\theta_{min} - \theta) dx + J(\theta). \quad (2.23)$$

Similar references [33], to solve the optimization problem, the Optimality Criteria algorithm is used here which can be written as:

$$\theta^{m+1} = \begin{cases} \max(0, \theta - move), & \text{if } \theta \beta^b \leq \max(0, \theta - move), \\ \min(1, \theta + move), & \text{if } \theta \beta^b \geq \min(1, \theta + move), \\ \theta \beta^b, & \text{otherwise,} \end{cases} \quad (2.24)$$

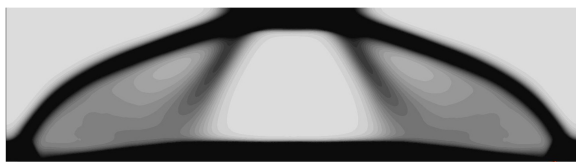
and $\beta = -\frac{\partial J}{\partial \theta} \left(\bar{\lambda} \frac{\partial V}{\partial \theta} \right)^{-1}$, where θ^{m+1} represents the value of the density variable in the iterative step $m = 1, 2, \dots, n$, *move* parameter is the maximum amount of density change, the value of *move* is considered to be 0.2, b is a damping coefficient and takes the value 0.3, $\bar{\lambda}$ is the Lagrange multiplier to augment the volume constrain.

Next, we introduce the optimization algorithm for the mechanical-electrical coupling problem of periodic composites as follows:

- 1). The geometric structure $Y = [0, 1]^2$ and homogenization domain Ω of the reference cell and the material parameters of each material were determined, the two domains are divided into finite element spaces $K^{h_1}(Y)$ and $K^{h_0}(Y)$, where h_1 and h_2 represent the mesh size of the monocellular domain and finite element respectively;
- 2). Equations (2.9) and (2.10) of first-order unicellular functions are solved on the finite element domain $K^{h_1}(Y)$, and obtain the first order monocellular solutions $M_{\alpha_1}(\xi)$, $H_{\alpha_1}(\xi)$, $N_{\alpha_1 m}(\xi)$ and $G_{\alpha_1 m}(\xi)$, and the coefficients of homogenization \hat{C}_{ijk}^θ , \hat{e}_{ijk}^θ and \hat{b}_{ij}^θ . Interpolation is performed using the calculated homogenization coefficients at these mesh points, finally, we can obtain the homogenization coefficients of domain $K^{h_0}(\Omega)$;
- 3). Substituting the homogenization coefficients \hat{C}_{ijk}^θ , \hat{e}_{ijk}^θ and \hat{b}_{ij}^θ into Eq (2.5) to find $\Phi^0(x)$ and $u_k^0(x)$;
- 4). By solving the adjoint Eq (2.12) of mechanical-electric coupling by finite element method, we can obtain $\chi_k(x)$ and $\phi(x)$;
- 5). Substituting $\Phi^0(x)$, $u^0(x)$, $\chi(x)$ and $\phi(x)$ into $J(\theta)$ and take the derivative of θ to obtain the sensitivity analysis (2.20);
- 6). In order to eliminate checkerboard and other problems, smoothing sensitivity (2.21) is used;
- 7). In order to obtain the optimal solution of the structure, it is necessary to continuously iterate and update the element density value, modify design variables using update scheme (2.23), here we use dichotomy to update the intermediate variable:
 - (a) Calculate the Lagrange multiplier $\Lambda = (\Lambda_{min} + \Lambda_{max})/2$, where Λ_{min} and Λ_{max} represent the upper limit and lower limit of the initial Kuhn-Tucker condition respectively, and substitute into (2.24) to update the design variable θ ;
 - (b) The structural volume $\int_{\Omega} \theta^{m+1} dx$ is calculated, if $\int_{\Omega} \theta^{m+1} dx - \int_{\Omega} \vartheta dx > 0$, output $\Lambda = \Lambda_{min}$, otherwise print $\Lambda = \Lambda_{max}$;
 - (c) Repeat (a) and (b) until $\Lambda_{max} > 10^{-40}$ and $(\Lambda_{max} - \Lambda_{min}) / (\Lambda_{min} + \Lambda_{max}) > 10^{-40}$, if true, output $\theta^{m+1} = \theta$, otherwise, go back to step (a).
- 8). Equations (2.1) and (2.2) were used to update the design variables for each material and calculate the average compliance and volume fraction as well as the variation of the variables;
- 9). Optimization convergence $|\theta^{m+1} - \theta^m| < 10^{-3}$, whether the number of iterations is greater than or equal to the maximum number of iterations, if so, output the result, otherwise return step (b).

3. Numerical results

In this section, we give some numerical results show that the proposed algorithm is effective to calculate the optimal structure of the periodic composite cantilever beam under the influence of the electromechanical coupling. Suppose a cantilever beams Ω with length $W = 2(m)$ and width $L = 0.5(m)$ were considered in the simulations. As shown in Figure 1, let Ω be a bounded domain with Lipschitz boundary. The boundary $\partial\Omega$ of Ω is composed of the traction boundary $B_t = \{x = -0.96 * l + 1.04, y = 0.625, l \in (0, 1)\}$ and the displacement boundary $B_u = \{x = 0.04 * l + 1.96, y = 0, l \in (0, 1)\}$, which do not overlap each other so that $B_u \cap B_t = \emptyset$ and $B_u \cup B_t = \partial\Omega$, a surface traction force $t_i(x) = -10^7(N)$ is applied to the border of B_t . Also consider the electrical boundary Ω is divided into two parts, the electric potential boundary $B_\phi = \{x = 0.08 * l + 0.96, y = 0, l \in (0, 1)\}$ and the electric loads boundary B_q , there are $B_\phi \cap B_q = \emptyset$ and $B_\phi \cup B_q = \partial\Omega$. $q(x) = 10^{-2}(C)$ denotes the electric body charge applied to the border B_ϕ of the design domain. Assume that $\gamma_i = 0.002$, $\lambda = 0.4$, $r = 0.1$, $\theta_{min} = 0.001$, $\Lambda_{min} = 0$, $\Lambda_{max} = 100,000$, $\vartheta = 0.4(m^3)$, the maximum number of iterations $n = 300$. And the Table 1 shows two different periodic composite material parameters.



a1. The 50th iteration of composite material.



b1. The 50th iteration of homogenization structure.



a2. The 100th iteration of composite material.



b2. The 100th iteration of homogenization structure.



a3. The 200th iteration of composite material.



b3. The 200th iteration of homogenization structure.



a4. The 300th iteration of composite material.



b4. The 300th iteration of homogenization structure.

Figure 2. The topological optimization of composite material and homogenization structure with 50–300 iterations.

Table 1. Material properties.

PZT5A(Y_1)	PZT4A (Y_2)	Homogenize material properties
$E_1 = 72 \times 10^9(N/m^2)$	$E_1 = 76 \times 10^9(N/m^2)$	$E_1 = 72 \times 10^9(N/m^2)$
$E_0 = E_1 10^{-9}(N/m^2)$	$E_0 = E_1 10^{-9}(N/m^2)$	$E_0 = E_1 10^{-9}(N/m^2)$
$e_{31} = -5.4(C/m^2)$	$e_{31} = -6.98(C/m^2)$	$e_{31} = -6.635(C/m^2)$
$e_{310} = e_{31} 10^{-9}(C/m^2)$	$e_{310} = e_{31} 10^{-9}(C/m^2)$	$e_{310} = e_{31} 10^{-9}(C/m^2)$
$e_{33} = 15.8(C/m^2)$	$e_{33} = 13.84(C/m^2)$	$e_{33} = 14.292(C/m^2)$
$e_{330} = e_{33} 10^{-9}(C/m^2)$	$e_{330} = e_{33} 10^{-9}(C/m^2)$	$e_{330} = e_{33} 10^{-9}(C/m^2)$
$e_{15} = 12.3(C/m^2)$	$e_{15} = 13.44(C/m^2)$	$e_{15} = 13.217(C/m^2)$
$e_{150} = e_{15} 10^{-9}(C/m^2)$	$e_{150} = e_{15} 10^{-9}(C/m^2)$	$e_{150} = e_{15} 10^{-9}(C/m^2)$
$b_{11} = 916(F/m)$	$b_{11} = 677(F/m)$	$b_{11} = 743.557(F/m)$
$b_{110} = b_{33} 10^{-9}(F/m)$	$b_{110} = b_{11} 10^{-9}(F/m)$	$b_{110} = b_{11} 10^{-9}(F/m)$
$b_{33} = 830(F/m)$	$b_{33} = 618(F/m)$	$b_{33} = 676.708(F/m)$
$b_{330} = b_{33} 10^{-9}(F/m)$	$b_{330} = b_{33} 10^{-9}(F/m)$	$b_{330} = b_{33} 10^{-9}(F/m)$

In order to illustrate the effectiveness of topology optimization algorithms using solid isotropic material penalization method and homogenization method, some numerical results of periodic composite topology optimization are presented. In other words, the comparison of the mechanical-electrical coupling topology optimization between the composite cantilever in fine mesh which is the reference solution of this problem and the homogeneous cantilever in coarse mesh is shown in Figure 2. It can be seen from a3 and a4 in Figure 2 that the topology optimization results of composite structures are almost unchanged after 200 and 300 iterations. Similarly, it can also be seen from b3 and b4 in Figure 2 that the topology optimization results of homogeneous cantilever are almost unchanged after 200 and 300 iterations. Therefore, this shows that the topology optimization algorithm of material structure is convergent after 300 iterations. It can be seen from a4 and b4 in Figure 2 that the topology optimization result of composite cantilever is consistent with the topology optimization result of homogeneous cantilever. Therefore, it is concluded that the homogeneity method can effectively obtain the topological optimization of the composite.

In the following Figure 3, it shows the convergence curve of the objective function. It can be seen from the curve change that the objective function value is decreasing fast in the first 100 iterations and almost unchanged after 200 iterations. In this paper, we take the topology optimization result of the structure at 300 iterations as the final result of the material structure design. This is consistent with the conclusion in Figure 2.

Table 2 shows the grid information of composite material and homogenization structure respectively. It can be seen from the table 2 that the number of triangles or vertices of the composite material is much greater than that of the homogenization structure. So it can be known that the calculation cost of the fine mesh method is much higher than that of the homogenization method. Therefore the topology optimization algorithm of piezoelectric composite structure based on homogenization theory is very effective.

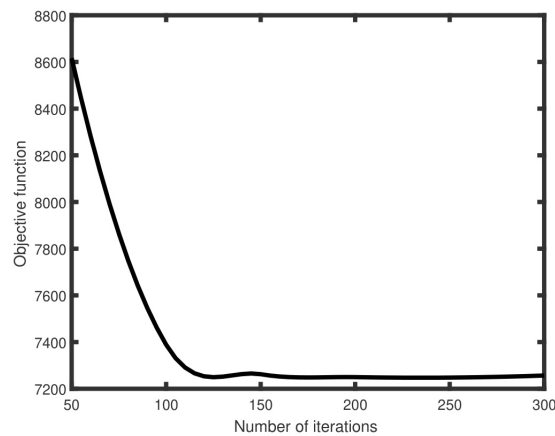


Figure 3. Convergence of objective functions.

Table 2. Grid information.

	Macro periodic complex solution	Homogenized solution
Triangles	1,207,779	191,601
vertices	606,690	96,851

4. Conclusions

In this paper, the topological optimization algorithm and numerical simulation for electro-mechanical coupling problems of composites are discussed. Using the two scale asymptotic method, we prove the homogenization problem of topological optimization electro-mechanical coupling problems of composites. By solving the homogenization problem of the topology optimization problem of the piezoelectric composite structure, we obtained the topology optimization algorithm of the topology optimization problem of the piezoelectric composite structure. The numerical results of the paper show that the results of equivalent homogenized materials are close to the results of calculating composite materials in fine mesh. Therefore the topology optimization algorithm of piezoelectric composite structure based on homogenization theory is effective. The structural optimization of piezoelectric materials has a broad application prospect, which can be used in intelligent sensors, intelligent control, intelligent robots, intelligent home, intelligent transportation and other fields. In addition, structural optimization of piezoelectric materials can also be used to improve the performance, reliability and energy efficiency of electronic components.

In the future work, we will use the topological optimization algorithm to establish the topology optimization algorithm of structural optimization of composite plates of electro-mechanical coupling problems.

Acknowledgments

Ziqiang Wang was supported by National Natural Science Foundation of China (Grant No. 11961009). Junying Cao was supported by National Natural Science Foundation of China (Grant No. 11901135), Foundation of Guizhou Science and Technology Department, China (Grant No. [2020]1Y015). Ziqiang Wang and Junying Cao were supported by Natural Science Research Project of Department of Education of Guizhou Province (Grant Nos. QJJ2022015 and QJJ2022047).

Conflict of interest

The authors declare there is no conflicts of interest.

References

1. A. C. Eringen, Theory of nonlocal piezoelectricity, *J. Math. Phys.*, **25** (1984), 717–727. <https://doi.org/10.1063/1.526180>
2. J. S. Yang, R. C. Batra, Conservation laws in linear piezoelectricity, *Eng. Fract. Mech.*, **51** (1995), 1041–1047. [https://doi.org/10.1016/0013-7944\(94\)00271-I](https://doi.org/10.1016/0013-7944(94)00271-I)
3. M. Deng, Y. Feng, Two-scale finite element for piezoelectric problem in periodic structure, *Appl. Math. Mech.*, **32** (2011), 1525–1540. <https://doi.org/10.1007/s10483-011-1521-7>
4. J. Telega, S. Bytner, Piezoelectricity with polarization gradient: homogenization, *Mech. Res. Commun.*, **29** (2002), 53–59. [https://doi.org/10.1016/S0093-6413\(02\)00228-8](https://doi.org/10.1016/S0093-6413(02)00228-8)
5. G. Allaire, E. Bonnetier, G. Francfort, F. Jouve, Shape optimization by the homogenization method, *Numer. Math.*, **76** (1997), 27–68. <https://doi.org/10.1007/s002110050253>
6. M. Zhou, D. Geng, Multi-scale and multi-material topology optimization of channel-cooling cellular structures for thermomechanical behaviors, *Comput. Methods Appl. Mech. Eng.*, **383** (2021), 113896. <https://doi.org/10.1016/j.cma.2021.113896>
7. X. Zhao, M. Zhou, Y. Liu, M. Ding, P. Hu, P. Zhu, Topology optimization of channel cooling structures considering thermomechanical behavior, *Struct. Multidiscip. Optim.*, **59** (2019), 613–632. <https://doi.org/10.1007/s00158-018-2087-z>
8. L. Ling, J. Yan, G. Cheng, Optimum structure with homogeneous optimum truss-like material, *Comput. Struct.*, **86** (2008), 1417–1425. <https://doi.org/10.1016/j.compstruc.2007.04.030>
9. A. Homayouni-Amlashi, A. Mohand-Ousaid, M. Rakotondrabe, Topology optimization of 2DOF piezoelectric plate energy harvester under external in-plane force, *J. Micro-Bio Rob.*, **16** (2020), 65–77. <https://doi.org/10.1007/s12213-020-00129-0>
10. B. Yang, C. Cheng, X. Wang, Z. Meng, A. Homayouni-Amlashi, Reliability-based topology optimization of piezoelectric smart structures with voltage uncertainty, *J. Intell. Mater. Syst. Struct.*, **33** (2022), 1975–1989. <https://doi.org/10.1177/1045389X211072197>
11. L. Xu, G. Cheng, Two-scale concurrent topology optimization with multiple micro materials based on principal stress orientation, *Struct. Multidiscip. Optim.*, **57** (2018), 2093–2107. <https://doi.org/10.1007/s00158-018-1916-4>

12. S. Xu, G. Cheng, Optimum material design of minimum structural compliance under seepage constraint, *Struct. Multidiscip. Optim.*, **41** (2010), 575–587. <https://doi.org/10.1007/s00158-009-0438-5>
13. H. Rodrigues, J. Guedes, M. Bendsoe, Hierarchical optimization of material and structure, *Struct. Multidiscip. Optim.*, **24** (2002), 1–10. <https://doi.org/10.1007/s00158-002-0209-z>
14. J. Guedes, N. Kikuchi, Preprocessing and postprocessing for materials based on the homogenization method with adaptive finite element methods, *Comput. Methods Appl. Mech. Eng.*, **83** (1990), 143–198. [https://doi.org/10.1016/0045-7825\(90\)90148-F](https://doi.org/10.1016/0045-7825(90)90148-F)
15. E. Andreassen, C. Andreasen, How to determine composite material properties using numerical homogenization, *Comput. Mater. Sci.*, **83** (2014), 488–495. <https://doi.org/10.1016/j.commatsci.2013.09.006>
16. G. Cheng, Y. Cai, L. Xu, Novel implementation of homogenization method to predict effective properties of periodic materials, *Acta Mech. Sin.*, **29** (2013), 550–556. <https://doi.org/10.1007/s10409-013-0043-0>
17. Y. Wang, M. Wang, F. Chen, Structure-material integrated design by level sets, *Struct. Multidiscip. Optim.*, **54** (2016), 1145–1156. <https://doi.org/10.1007/s00158-016-1430-5>
18. J. Guest, J. Prvost, Optimizing multifunctional materials: design of microstructures for maximized stiffness and fluid permeability, *Int. J. Solids Struct.*, **43** (2006), 7028–7047. <https://doi.org/10.1016/j.ijsolstr.2006.03.001>
19. J. Guest, J. Prvost, Design of maximum permeability material structures, *Comput. Methods Appl. Mech. Eng.*, **196** (2007), 1006–1017. <https://doi.org/10.1016/j.cma.2006.08.006>
20. Z. Han, Z. Wang, K. Wei, Shape morphing structures inspired by multi-material topology optimized bi-functional metamaterials, *Compos. Struct.*, **300** (2022), 116135. <https://doi.org/10.1016/j.compstruct.2022.116135>
21. Z. Han, K. Wei, Multi-material topology optimization and additive manufacturing for metamaterials incorporating double negative indexes of Poissons ratio and thermal expansion, *Addit. Manuf.*, **54** (2022), 102742. <https://doi.org/10.1016/j.addma.2022.102742>
22. M. Costa, A. Sohoulis, A. Suleman, Multi-scale and multi-material topology optimization of gradient lattice structures using surrogate models, *Compos. Struct.*, **289** (2022), 115402. <https://doi.org/10.1016/j.compstruct.2022.115402>
23. X. Huangy, W. Li, A new multi-material topology optimization algorithm and selection of candidate materials, *Comput. Methods Appl. Mech. Eng.*, **386** (2021), 114114. <https://doi.org/10.1016/J.CMA.2021.114114>
24. Z. Wang, J. Cui, Second-order two-scale method for bending behavior analysis of composite plate with 3-D periodic configuration and its approximation, *Sci. China Math.*, **57** (2014), 1713–1732. <https://doi.org/10.1007/s11425-014-4831-1>
25. J. Cao, C. Xu, A high order schema for the numerical solution of the fractional ordinary differential equations, *J. Comput. Phys.*, **238** (2013), 154–168. <https://doi.org/10.1016/j.jcp.2012.12.013>

26. L. Tian, Z. Wang, J. Cao, A high-order numerical scheme for right Caputo fractional differential equations with uniform accuracy, *Electron. Res. Arch.*, **30** (2022), 3825–3854. [https://doi:10.3934/era.2022195](https://doi.org/10.3934/era.2022195)
27. C. Wang, J. Zhu, W. Zhang, S. Li, J. Kong, Concurrent topology optimization design of structures and non-uniform parameterized lattice microstructures, *Struct. Multidiscip. Optim.*, **58** (2018), 35–50. <https://doi.org/10.1007/s00158-018-2009-0>
28. P. Gangl, A multi-material topology optimization algorithm based on the topological derivative, *Comput. Methods Appl. Mech. Eng.*, **366** (2020), 113090. <https://doi.org/10.1016/j.cma.2020.113090>
29. Y. Feng, M. Deng, X. Guan, The twoscale asymptotic error analysis for piezoelectric problems in the quasi-periodic structure, *Sci. China Phys., Mech. Astron.*, **56** (2013), 1844–1853. <https://doi.org/10.1007/s11433-013-5304-1>
30. A. Homayouni-Amlashi, T. Schlinquer, A. Mohand-Ousaid, M. Rakotondrabe, 2D topology optimization MATLAB codes for piezoelectric actuators and energy harvester, *Struct. Multidiscip. Optim.*, **63** (2021), 983–1014. <https://doi.org/10.1007/s00158-020-02726-w>
31. M. Wang, S. Feng, A. Incecik, G. Krolczyk, Z. Li, Structural fatigue life prediction considering model uncertainties through a novel digital twin-driven approach, *Comput. Methods Appl. Mech. Eng.*, **391** (2022), 114512. <https://doi.org/10.1016/j.cma.2021.114512>
32. S. Feng, X. Han, Z. Li, A. Incecik, Ensemble learning for remaining fatigue life prediction of structures with stochastic parameters: a data-driven approach, *Appl. Math. Modell.*, **101** (2022), 420–431. <https://doi.org/10.1016/j.apm.2021.08.033>
33. W. Mason, H. Baerwald, Piezoelectric crystals and their applications to ultrasonics, *Phys. Today*, **4** (1951), 23–24. <https://doi.org/10.1063/1.3067231>

Appendix

Appendix A: the proof of Theorem 2.1.

Proof. The asymptotic expansion of $\Phi^\varepsilon(x)$ and $u_k^\varepsilon(x)$ is as follows:

$$\Phi^\varepsilon(x) = \Phi(x, x/\varepsilon) = \Phi(x, \xi) = \Phi^0(x, \xi) + \varepsilon\Phi^1(x, \xi) + \varepsilon^2\Phi^2(x, \xi) + o(\varepsilon^2), \quad (\text{A.1})$$

$$u_k^\varepsilon(x) = u_k(x, x/\varepsilon) = u_k(x, \xi) = u_k^0(x, \xi) + \varepsilon u_k^1(x, \xi) + \varepsilon^2 u_k^2(x, \xi) + o(\varepsilon^2), \quad (\text{A.2})$$

in which x and ξ are two independent variables, and the partial derivative operation is:

$$\frac{\partial}{\partial x_i} \rightarrow \frac{\partial}{\partial x_i} + \varepsilon^{-1} \frac{\partial}{\partial \xi_i}. \quad (\text{A.3})$$

Suppose $\Phi^j(x, \xi)$ and $u^j(x, \xi)$ ($j = 0, 1, 2$), $x \in \Omega$, $\xi \in Y$ are Y -periodic with respect to ξ . Define the operators H_ε , F_ε , A_ε and W_ε as follows:

$$H^\varepsilon = -\frac{\partial}{\partial x_j} (C_{ijkl}^\theta(\xi) \frac{\partial}{\partial x_l}), \quad F^\varepsilon = -\frac{\partial}{\partial x_j} (e_{kij}^\theta(\xi) \frac{\partial}{\partial x_k}),$$

$$A^\varepsilon = -\frac{\partial}{\partial x_i} (b_{ij}^\theta(\xi) \frac{\partial}{\partial x_j}), \quad W^\varepsilon = \frac{\partial}{\partial x_i} (e_{kij}^\theta(\xi) \frac{\partial}{\partial x_j}).$$

Form (2.4), the mechanical-electrical coupling equations can be written as:

$$\begin{aligned} f_k(x)\theta(x) &= H^\varepsilon u_k^\varepsilon + F^\varepsilon \Phi^\varepsilon \\ &= (\varepsilon^{-2} H_0 + \varepsilon^{-1} H_1 + H_2) (u_k^0 + \varepsilon u_k^1 + \varepsilon^2 u_k^2 + o(\varepsilon^2)) (x, x/\varepsilon) \\ &\quad + (\varepsilon^{-2} F_0 + \varepsilon^{-1} F_1 + F_2) (\Phi^0 + \varepsilon \Phi^1 + \varepsilon^2 \Phi^2 + o(\varepsilon^2)) (x, x/\varepsilon), \end{aligned} \quad (\text{A.4})$$

$$\begin{aligned} \rho(x)\theta(x) &= W^\varepsilon u_k^\varepsilon + A^\varepsilon \Phi^\varepsilon \\ &= (\varepsilon^{-2} W_0 + \varepsilon^{-1} W_1 + W_2) (u_k^0 + \varepsilon u_k^1 + \varepsilon^2 u_k^2 + o(\varepsilon^2)) (x, x/\varepsilon) \\ &\quad + (\varepsilon^{-2} A_0 + \varepsilon^{-1} A_1 + A_2) (\Phi^0 + \varepsilon \Phi^1 + \varepsilon^2 \Phi^2 + o(\varepsilon^2)) (x, x/\varepsilon), \end{aligned} \quad (\text{A.5})$$

where

$$\left\{ \begin{aligned} H_0 &= -\frac{\partial}{\partial \xi_j} (C_{ijkl}^\theta(\xi) \frac{\partial}{\partial \xi_l}), \quad H_1 = -\frac{\partial}{\partial \xi_j} (C_{ijkl}^\theta(\xi) \frac{\partial}{\partial x_l}) - \frac{\partial}{\partial x_j} (C_{ijkl}^\theta(\xi) \frac{\partial}{\partial \xi_l}), \\ H_2 &= -\frac{\partial}{\partial x_j} (C_{ijkl}^\theta(\xi) \frac{\partial}{\partial x_l}), \quad F_0 = -\frac{\partial}{\partial \xi_j} (e_{kij}^\theta(\xi) \frac{\partial}{\partial \xi_k}), \\ F_1 &= -\frac{\partial}{\partial \xi_j} (e_{kij}^\theta(\xi) \frac{\partial}{\partial x_k}) - \frac{\partial}{\partial x_j} (e_{kij}^\theta(\xi) \frac{\partial}{\partial \xi_k}), \quad F_2 = -\frac{\partial}{\partial x_j} (e_{kij}^\theta(\xi) \frac{\partial}{\partial x_k}), \\ A_0 &= -\frac{\partial}{\partial \xi_i} (b_{ij}^\theta(\xi) \frac{\partial}{\partial \xi_j}), \quad A_1 = -\frac{\partial}{\partial \xi_i} (b_{ij}^\theta(\xi) \frac{\partial}{\partial x_j}) - \frac{\partial}{\partial x_i} (b_{ij}^\theta(\xi) \frac{\partial}{\partial \xi_j}), \\ A_2 &= -\frac{\partial}{\partial x_i} (b_{ij}^\theta(\xi) \frac{\partial}{\partial x_j}), \quad W_0 = \frac{\partial}{\partial \xi_i} (e_{ijk}^\theta(\xi) \frac{\partial}{\partial \xi_j}), \\ W_1 &= \frac{\partial}{\partial \xi_i} (e_{ijk}^\theta(\xi) \frac{\partial}{\partial x_j}) + \frac{\partial}{\partial x_i} (e_{ijk}^\theta(\xi) \frac{\partial}{\partial \xi_j}), \quad W_2 = \frac{\partial}{\partial x_i} (e_{ijk}^\theta(\xi) \frac{\partial}{\partial x_j}). \end{aligned} \right. \quad (\text{A.6})$$

By comparing the ε power coefficients at both ends of Eqs (A.4) and (A.5), (A.1) and (A.2), we can obtain the following equations:

$$\left\{ \begin{aligned} H_0 u_k^0 &= -F_0 \Phi^0, \quad A_0 \Phi^0 = -W_0 u_k^0, \quad \text{in } Y, \\ u_k^0 \text{ and } \Phi^0 &\text{ for } \xi \text{ is the period } Y. \end{aligned} \right. \quad (\text{A.7})$$

$$\left\{ \begin{aligned} H_0 u_k^1 &= -F_0 \Phi^1 - F_1 \Phi^0 - H_1 u_k^0, \quad \text{in } Y, \\ A_0 \Phi^1 &= -A_1 \Phi^0 - W_0 u_k^1 - W_1 u_k^0, \quad \text{in } Y, \\ u_k^1 \text{ and } \Phi^1 &\text{ for } \xi \text{ is the period } Y. \end{aligned} \right. \quad (\text{A.8})$$

$$\left\{ \begin{aligned} H_0 u_k^2 &= f_k(x)\theta(x) - H_1 u_k^1 - H_2 u_k^0 - F_0 \Phi^2 - F_1 \Phi^1 - F_2 \Phi^0, \quad \text{in } Y, \\ A_0 \Phi^2 &= \rho(x)\theta(x) - A_1 \Phi^1 - A_2 \Phi^0 - W_0 u_k^2 - W_1 u_k^1 - W_2 u_k^0, \quad \text{in } Y, \\ u_k^2 \text{ and } \Phi^2 &\text{ for } \xi \text{ is the period } Y. \end{aligned} \right. \quad (\text{A.9})$$

For Eq (A.7), we can be further expressed is:

$$\frac{\partial}{\partial \xi_j} \left(e_{kij}^\theta(\xi) \frac{\partial \Phi^0}{\partial \xi_k} \right) + \frac{\partial}{\partial \xi_j} \left(C_{ijkl}^\theta(\xi) \frac{\partial u_k^0}{\partial \xi_l} \right) = 0, \quad (\text{A.10})$$

$$\frac{\partial}{\partial \xi_i} \left(e_{ijk}^\theta(\xi) \frac{\partial u_k^0}{\partial \xi_j} \right) - \frac{\partial}{\partial \xi_i} \left(b_{ij}^\theta(\xi) \frac{\partial \Phi^0}{\partial \xi_j} \right) = 0. \quad (\text{A.11})$$

According to the theory of partial differential equation, both $\Phi^0(x, \xi)$ and $u_k^0(x, \xi)$ are independent of microscopic variable ξ , i.e.,

$$\Phi^0(x, \xi) = \Phi^0(x), u_k^0(x, \xi) = u_k^0(x). \quad (\text{A.12})$$

Substituting (A.12) into (A.8) yields:

$$\left\{ \begin{array}{l} - \left(\frac{\partial}{\partial \xi_j} (C_{ijkl}^\theta(\xi) \frac{\partial u_k^1}{\partial \xi_l}) + \frac{\partial}{\partial \xi_j} (e_{kij}^\theta(\xi) \frac{\partial \Phi^1}{\partial \xi_k}) \right) = \frac{\partial C_{ijkl}^\theta(\xi)}{\partial \xi_j} \frac{\partial u_k^0}{\partial x_l} + \frac{\partial e_{kij}^\theta(\xi)}{\partial \xi_j} \frac{\partial \Phi^0}{\partial x_k}, \\ - \left(\frac{\partial}{\partial \xi_i} (b_{ij}^\theta(\xi) \frac{\partial \Phi^1}{\partial \xi_j}) - \frac{\partial}{\partial \xi_i} (e_{ijk}^\theta(\xi) \frac{\partial u_k^1}{\partial \xi_j}) \right) = \frac{\partial b_{ij}^\theta(\xi)}{\partial \xi_i} \frac{\partial \Phi^0}{\partial x_j} - \frac{\partial e_{ijk}^\theta(\xi)}{\partial \xi_i} \frac{\partial u_k^0}{\partial x_j}, \\ \Phi^1 \text{ and } u_k^1 \text{ for } \xi \text{ is the period } Y. \end{array} \right. \quad (\text{A.13})$$

By the linear property of (A.12), the operators H_0, F_0, W_0 and A_0 refer only to the variable ξ , and the partial derivative operations $\frac{\partial \Phi^0}{\partial x_j}$ and $\frac{\partial u_k^0}{\partial x_j}$ are independent of ξ , so it can be solved in the following form

$$\left\{ \begin{array}{l} \Phi^1(x, \xi) = H_\alpha(\xi) \frac{\partial \Phi^0(x)}{\partial x_\alpha} + G_{\alpha m}(\xi) \frac{\partial u_m^0(x)}{\partial x_\alpha}, \\ u^1(x, \xi) = N_\alpha(\xi) \frac{\partial u^0(x)}{\partial x_\alpha} + M_\alpha(\xi) \frac{\partial \Phi^0(x)}{\partial x_\alpha}. \end{array} \right. \quad (\text{A.14})$$

Substituting (A.14) into (A.13), which leads to

$$\left\{ \begin{array}{l} \frac{\partial}{\partial \xi_j} \left(e_{kij}^\theta(\xi) \frac{\partial H_{\alpha_1}(\xi)}{\partial \xi_k} \right) + \frac{\partial}{\partial \xi_j} \left(C_{ijhk}^\theta(\xi) \frac{\partial (M_{\alpha_1}(\xi))_h}{\partial \xi_k} \right) = - \frac{\partial}{\partial \xi_j} \left(e_{\alpha_1 ij}^\theta(\xi) \right), \text{ in } \Omega, \\ \frac{\partial}{\partial \xi_i} \left(-b_{ij}^\theta(\xi) \frac{\partial H_{\alpha_1}(\xi)}{\partial \xi_j} \right) + \frac{\partial}{\partial \xi_i} \left(e_{ijk}^\theta(\xi) \frac{\partial (M_{\alpha_1}(\xi))_k}{\partial \xi_j} \right) = \frac{\partial}{\partial \xi_i} \left(b_{\alpha_1 i}^\theta(\xi) \right), \text{ in } \Omega, \\ \int_{\Omega} M_{\alpha_1}(\xi) d\xi = 0, \int_{\Omega} H_{\alpha_1}(\xi) d\xi = 0, M_{\alpha_1}(\xi), H_{\alpha_1}(\xi) \text{ is } Y\text{-periodic in } \xi, \end{array} \right. \quad (\text{A.15})$$

and

$$\left\{ \begin{array}{l} \frac{\partial}{\partial \xi_j} \left(e_{kij}^\theta(\xi) \frac{\partial G_{\alpha_1 m}(\xi)}{\partial \xi_k} \right) + \frac{\partial}{\partial \xi_j} \left(C_{ijhk}^\theta(\xi) \frac{\partial (N_{\alpha_1 m}(\xi))_h}{\partial \xi_k} \right) = - \frac{\partial}{\partial \xi_j} \left(C_{ij\alpha_1 m}^\theta(\xi) \right), \text{ in } \Omega, \\ \frac{\partial}{\partial \xi_i} \left(-b_{ij}^\theta(\xi) \frac{\partial G_{\alpha_1 m}(\xi)}{\partial \xi_j} \right) + \frac{\partial}{\partial \xi_i} \left(e_{ijk}^\theta(\xi) \frac{\partial (N_{\alpha_1 m}(\xi))_k}{\partial \xi_j} \right) = - \frac{\partial}{\partial \xi_i} \left(e_{i m \alpha_1}^\theta(\xi) \right), \text{ in } \Omega, \\ \int_{\Omega} N_{\alpha_1 m}(\xi) d\xi = 0, \int_{\Omega} G_{\alpha_1 m}(\xi) d\xi = 0, N_{\alpha_1 m}(\xi), G_{\alpha_1 m}(\xi) \text{ is } Y\text{-periodic in } \xi. \end{array} \right. \quad (\text{A.16})$$

Suppose these three the homogenization coefficients $\hat{C}_{ijk}^\theta, \hat{e}_{ijk}^\theta$ and \hat{b}_{ij}^θ satisfy conditions (I)-(IV), $\Phi^\varepsilon(x) \in Z = \{\Phi(x) \in H^1(\Omega) \mid \Phi(x) = 0 \text{ on } B_i\}$, $u_k^\varepsilon(x) \in U = \{u_k(x) \in [H^1(\Omega)]^2 \mid u_k(x) = 0 \text{ on } B_u\}$, so the

monocellular problems (A.15) and (A.16) have unique solutions $M_{\alpha_1}(\xi)$, $H_{\alpha_1}(\xi)$, $N_{\alpha_1 m}(\xi)$ and $G_{\alpha_1 m}(\xi) \in W_{per}(Y)$, where $W_{per}(Y) = \{\theta(\xi) \mid \theta(\xi) \in H^1(\Omega)\}$, and $\theta(\xi)$ is periodic Y .

All operators of formula (A.9) are expanded as follows:

$$\begin{aligned} -\frac{\partial}{\partial \xi_j} \left(C_{ijkl}^\theta(\xi) \frac{\partial u_k^2}{\partial \xi_l} + e_{kij}^\theta(\xi) \frac{\partial \Phi^2}{\partial \xi_k} \right) &= \frac{\partial}{\partial \xi_j} \left(C_{ijkl}^\theta(\xi) \frac{\partial u_k^1}{\partial x_l} + e_{kij}^\theta(\xi) \frac{\partial \Phi^1}{\partial x_k} \right) \\ &+ \frac{\partial}{\partial x_j} \left(C_{ijkl}^\theta(\xi) \frac{\partial u_k^1}{\partial \xi_l} + C_{ijkl}^\theta(\xi) \frac{\partial u_k^0}{\partial x_l} \right) + \frac{\partial}{\partial x_j} \left(e_{kij}^\theta(\xi) \frac{\partial \Phi^1}{\partial \xi_k} + e_{kij}^\theta(\xi) \frac{\partial \Phi^0}{\partial x_k} \right) + f_i(x)\theta(x), \end{aligned} \quad (A.17)$$

$$\begin{aligned} -\frac{\partial}{\partial \xi_i} b_{ij}^\theta(\xi) \frac{\partial \Phi^2}{\partial \xi_j} + \frac{\partial}{\partial \xi_i} e_{ijk}^\theta(\xi) \frac{\partial u_k^2}{\partial \xi_j} &= \frac{\partial}{\partial \xi_i} \left(b_{ij}^\theta(\xi) \frac{\partial \Phi^1}{\partial x_j} - e_{ijk}^\theta(\xi) \frac{\partial u_k^1}{\partial x_j} \right) \\ &+ \frac{\partial}{\partial x_i} \left(b_{ij}^\theta(\xi) \frac{\partial \Phi^1}{\partial \xi_j} + b_{ij}^\theta(\xi) \frac{\partial \Phi^0}{\partial x_j} \right) - \frac{\partial}{\partial x_i} \left(e_{ijk}^\theta(\xi) \frac{\partial u_k^1}{\partial \xi_j} - e_{ijk}^\theta(\xi) \frac{\partial u_k^0}{\partial x_j} \right) + \rho(x)\theta(x). \end{aligned} \quad (A.18)$$

For Eqs (A.17) and (A.18), you average the integral over Y , according to the definition (A.14) of $\Phi^1(x)$ and $u_k^1(x)$, and the Y periodicity of $\Phi^2(x)$ and $u_k^2(x)$ on ξ , Eqs (A.17) and (A.18) can still be written as:

$$\begin{aligned} -\frac{\partial}{\partial x_j} \left\{ \frac{1}{|Y|} \int_Y \left(C_{ijlm}^\theta(\xi) \frac{\partial (N_{hk}(\xi))_l}{\partial \xi_m} + C_{ijhk}^\theta(\xi) + e_{lij}^\theta(\xi) \frac{\partial G_{hk}(\xi)}{\partial \xi_l} \right) d\xi \frac{\partial u_k^0(x)}{\partial x_h} \right. \\ \left. + \frac{1}{|Y|} \int_Y \left(C_{ijlm}^\theta(\xi) \frac{\partial (M_k(\xi))_l}{\partial \xi_m} + e_{lij}^\theta(\xi) \frac{\partial H_k(\xi)}{\partial \xi_l} + e_{ijk}^\theta(\xi) \right) d\xi \frac{\partial \Phi^0(x)}{\partial x_k} \right\} &= f_i(x)\theta(x), \quad \text{in } \Omega, \end{aligned} \quad (A.19)$$

$$\begin{aligned} -\frac{\partial}{\partial x_i} \left\{ \frac{1}{|Y|} \int_Y \left(b_{ij}^\theta(\xi) + b_{ik}^\theta(\xi) \frac{\partial H_j(\xi)}{\partial \xi_k} - e_{ilm}^\theta(\xi) \frac{\partial (M_j(\xi))_m}{\partial \xi_l} \right) d\xi \frac{\partial \Phi^0(x)}{\partial x_j} \right. \\ \left. - \frac{1}{|Y|} \int_Y \left(e_{ijk}^\theta(\xi) + e_{ilm}^\theta(\xi) \frac{\partial (N_{kj}(\xi))_m}{\partial \xi_l} - b_{il}^\theta(\xi) \frac{\partial G_{kj}(\xi)}{\partial \xi_l} \right) d\xi \frac{\partial u_k^0(x)}{\partial x_j} \right\} &= \rho(x)\theta(x), \quad \text{in } \Omega. \end{aligned} \quad (A.20)$$

Therefore, the homogenization equations are defined as:

$$-\frac{\partial}{\partial x_j} \left(\hat{C}_{ijkl}^\theta \frac{\partial u_k^0(x)}{\partial x_l} + \hat{e}_{kij}^\theta \frac{\partial \Phi^0(x)}{\partial x_k} \right) = f_i(x)\theta(x), \quad -\frac{\partial}{\partial x_i} \left(\hat{b}_{ij}^\theta \frac{\partial \Phi^0(x)}{\partial x_j} - \hat{e}_{ijk}^\theta \frac{\partial u_k^0(x)}{\partial x_j} \right) = \rho(x)\theta(x), \quad \text{in } \Omega,$$

where \hat{C}_{ijkl}^θ , \hat{e}_{kij}^θ and \hat{b}_{ij}^θ are homogenization coefficients, which can be expressed as:

$$\begin{cases} \hat{C}_{ijhk}^\theta = \frac{1}{|Y|} \int_Y \left[C_{ijhk}^\theta(\xi) + C_{ijlm}^\theta(\xi) \frac{\partial (N_{hk}(\xi))_m}{\partial \xi_l} + e_{lij}^\theta(\xi) \frac{\partial G_{hk}(\xi)}{\partial \xi_l} \right] d\xi, \\ \hat{e}_{ijk}^\theta = \frac{1}{|Y|} \int_Y \left[e_{ijk}^\theta(\xi) + C_{ijlm}^\theta(\xi) \frac{\partial (M_k(\xi))_m}{\partial \xi_l} + e_{lij}^\theta(\xi) \frac{\partial H_k(\xi)}{\partial \xi_l} \right] d\xi, \\ \hat{b}_{ij}^\theta = \frac{1}{|Y|} \int_Y \left[b_{ij}^\theta(\xi) - e_{ilm}^\theta(\xi) \frac{\partial (M_j(\xi))_m}{\partial \xi_l} + b_{ik}^\theta(\xi) \frac{\partial H_j(\xi)}{\partial \xi_k} \right] d\xi. \end{cases} \quad (A.21)$$

Substituting (A.1) and (A.2) into (2.3) of the objective function, the minimization of mechanical-electrical coupling problem (2.3) can be rewritten as:

$$\begin{aligned} \min_{\theta} J(\theta) &= \int_{\Omega} f_i(x) \left[u_i^0(x, \xi) + \varepsilon u_i^1(x, \xi) + \varepsilon^2 u_i^2(x, \xi) + o(\varepsilon^2) \right] \theta(x) dx \\ &+ \int_{B_i} t_i(x) \left[u_i^0(x, \xi) + \varepsilon u_i^1(x, \xi) + \varepsilon^2 u_i^2(x, \xi) + o(\varepsilon^2) \right] ds \\ &- \int_{\Omega} \rho(x) \left[\Phi^0(x, \xi) + \varepsilon \Phi^1(x, \xi) + \varepsilon^2 \Phi^2(x, \xi) + o(\varepsilon^2) \right] \theta(x) dx \\ &- \int_{B_{\phi}} q(x) \left[\Phi^0(x, \xi) + \varepsilon \Phi^1(x, \xi) + \varepsilon^2 \Phi^2(x, \xi) + o(\varepsilon^2) \right] ds. \end{aligned}$$

Assume that $\varepsilon \rightarrow 0$, because of $u_k^0(x, \xi)$ and $\Phi^0(x, \xi)$ are independent of ξ , the objective function of homogenization can be defined as:

$$\min_{\theta} J(\theta) = \int_{\Omega} f_i(x) u_i^0(x) \theta(x) dx + \int_{B_i} t_i(x) u_i^0(x) ds - \int_{\Omega} \rho(x) \Phi^0(x) \theta(x) dx - \int_{B_{\phi}} q(x) \Phi^0(x) ds.$$

The homogenization solution of $\Phi^0(x)$ and $u_k^0(x)$ satisfies the homogenization problem (2.5), so Theorem 2.1 is proved.



AIMS Press

© 2023 the Author(s), licensee AIMS Press. This is an open access article distributed under the terms of the Creative Commons Attribution License (<http://creativecommons.org/licenses/by/4.0>)